International Journal of Biological Macromolecules 44 (2009) 86–91

Contents lists available at ScienceDirect

International Journal of Biological Macromolecules

journal homepage: www.elsevier.com/locate/ijbiomac

Chemical force mapping of phosphate and carbon on acid-modified tapioca starch surface

Karntarat Wuttisela[a], Wannapong Triampo[b], Darapond Triampo[c,*]

[a] Institute for Innovation and Development of Learning Process, Mahidol University, Salaya Campus, Phuttamonthon Sai 4 Rd., Nakhon Pathom 73170, Thailand
[b] R&D Group of Biological and Environmental Physics (BIOPHYSICS), Department of Physics, and Center of Excellence for Vectors and Vector-Borne Diseases, Faculty of Science, Mahidol University, Salaya Campus, Phuttamonthon Sai 4 Rd., Nakhon Pathom 73170, Thailand
[c] Department of Chemistry (R3/1), Capability Building Research Unit for Alternative, and Center of Excellence for Innovation in Chemistry, Faculty of Science, Mahidol University, Salaya Campus, Phuttamonthon Sai 4 Rd., Nakhon Pathom 73170, Thailand

ARTICLE INFO

Article history:
Received 21 July 2008
Received in revised form 16 October 2008
Accepted 17 October 2008
Available online 30 October 2008

Keywords:
Acid hydrolysis
Amylopectin
Amylose
Scanning chemical force microscopy (SCFM)
Phosphate
Carbon

ABSTRACT

Surface chemical microstructure of hydrochloric acid hydrolyzed tapioca starch producing different amylose:amylopectin (Am:Ap) ratios were studied with scanning chemical force microscopy (CFM). The chemical force probes were functionalized of two types with –OH (phosphate specific) and $–CH_3$ (carbon specific). Lateral force trace-minus-retrace (TMR) images from –OH and $–CH_3$ probes revealed changes in the phosphate domains and the carbon backbone for the varying acid hydrolyzed tapioca starch compared to that of the native tapioca starch. Scanning electron micrographs (SEM) showed different degree of the granule surface disruption before and after hydrolysis. The exterior structures of the acid hydrolyzed starch granules were chemically investigated with CFM to study the relationships of the surface molecular structures and the Am:Ap ratios.

1. Introduction

Acid-modified starch is one of the major ways to add value to tapioca starch. Medicinal tablet production using acid hydrolyzed starch by a direct compression process is used in the pharmaceutical industry [1–5]. Acid hydrolysis of starch below the gelatinization temperature is done to increase the relative crystallinity of the starch granules [4–10]. Acid preferentially hydrolyzes amorphous regions, while the crystalline regions remain intact. Amylose:amylopectin (Am:Ap) ratio can be altered under different acid hydrolysis conditions [7–10]. Native tapioca starch tablets have lower crushing strength than those from acid-modified preparations [5,11]. The increase in crushing strength of acid-modified starch results from the increased in crystallinity of the granules.

Although there have been a number of studies using scanning force microscopy (SFM) to study the structure of starch granules [12–14], systematic investigations of the *exterior surface* of acid hydrolyzed starch granules are more limited [15–19]. Exterior surfaces of the starch granules can play an important role in defining their chemical properties and modifications [20–24]. A branch of SFM where the SFM probe is chemically modified to have specific functional group is known as scanning chemical force microscopy (CFM). CFM is an applied concept of lateral force microscopy (LFM), also known as frictional force microscopy (FFM). The *molecular friction* is measured from the lateral twisting of the cantilever rather than the normal up and down deflection in SFM (Fig. 1). *Molecular friction* results from the probe–specimen interaction. Probe having specific functional group, such as, –OH and $–CH_3$, would be able to detect for hydrophobic/hydrophilic interactions [25] or specific chemical domains, such as, the phosphate/phosphorus [26], amine/amide/nitrogen [26,27], or carbon backbone [26,27] of the surface. The functionalized probe would exhibit higher interaction (*molecular frictional interaction*) to specific domains on the specimen surface [25–29]. Phosphate content has been correlated to the relative crystallinity of acid-modified starch [5,30]. Phosphate in native tapioca starch is primarily found in amylopectin clusters [5,30–34]. By chemically modifying the CFM probe with –OH and $–CH_3$ functional group, we expect to probe the phosphate domain with the –OH probe, and the carbon backbone with the $–CH_3$ probe of the granule exterior surfaces.

* Corresponding author. Tel.: +662 441 9817x1143; fax: +662 889 2337.
E-mail address: scdar@mahidol.ac.th (D. Triampo).

0141-8130/$ – see front matter © 2008 Elsevier B.V. All rights reserved.
doi:10.1016/j.ijbiomac.2008.10.005

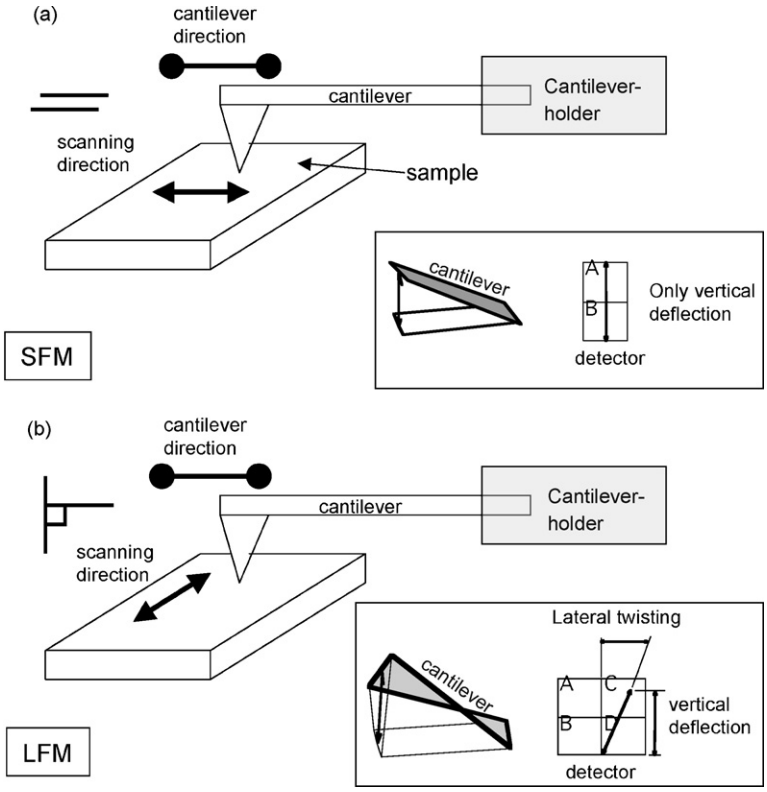

Fig. 1. (a) Scanning parallel to the direction to which the cantilever is held results in only the vertical deflection of the cantilever in SFM. (b) Lateral twisting of the cantilever result from scanning the sample at 90° to the direction to which the cantilever is held in LFM.

In this work, we have employed the use of functionalized $-CH_3$ and –OH probes to investigate the surface phosphate domain and carbon backbone of the exterior structures of acid hydrolyzed starch granules in order to study the relationships of the surface molecular structures and the Am:Ap ratios.

2. Experimental

2.1. Materials

Tapioca starch was obtained from a commercial source in Thailand. HCl, NaOH, trichlorooctadecylsilane (silane, $C_{18}H_{37}SiCl_3$), 30% H_2O_2, 98% H_2SO_4, and toluene were purchased from Merck KG, Darmstadt, Germany. Potassium iodide, iodine, acetic acid, pure potato amylose, ethanol, and paraffin wax were purchased from Sigma Co., Ltd., USA. Silicon nitride

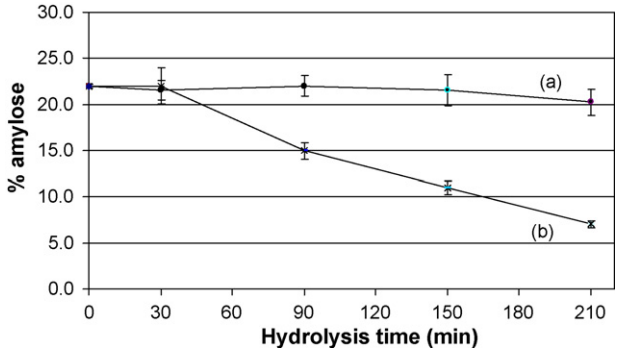

Fig. 2. Percent amylose after various hydrolysis times of (a) 0.7 M and (b) 2.0 M HCl.

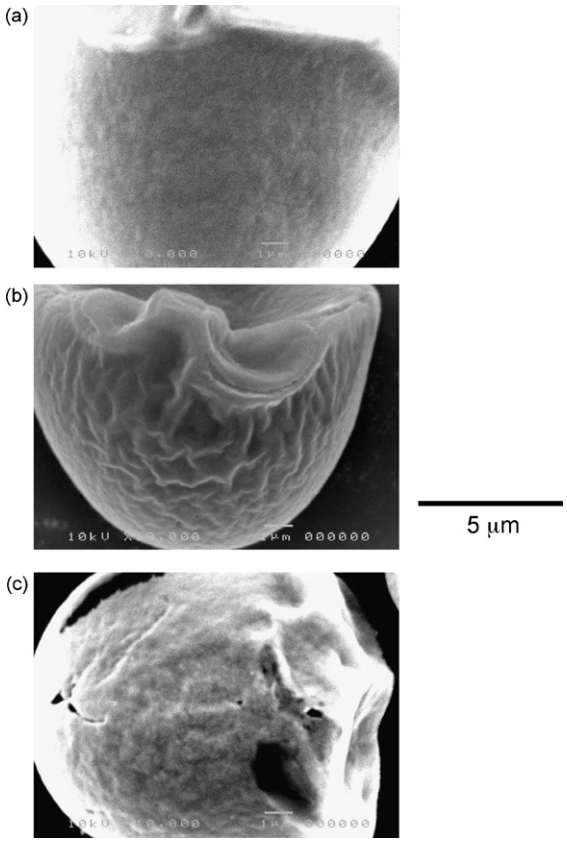

Fig. 3. SEM micrographs of tapioca starch: (a) native, (b) 0.7 M, and (c) 2.0 M HCl.

probe-cantilever assemblies were purchased from Veeco Store, USA.

2.2. Preparation of acid hydrolyzed tapioca starch

Ten percent (w/v) starch was suspended in 0.7 M or 2.0 M HCl for 3.5 h at 50 °C. The suspension was then neutralized to pH of 7.0 ± 0.5 with 0.05 M NaOH and washed several times with deionized water. Acid-modified starch was sedimented by centrifugation and was lyophilized. Amylose content of tapioca starch (based on dry weight) was determined by iodine affinity method using potato amylose as standard [30,35].

2.3. Granule surface disruption: scanning electron microscopy

The surface morphology of native tapioca starch and hydrolyzed starch was studied using a SEM (JEOL JSM-5310, Hert, UK) with 10 kV accelerating voltage and 10,000× magnification. The specimens were coated with thin film of gold for conductivity. The micrographs showed typical granule surfaces before and after acid hydrolysis. At least 20 micrographs of different granules

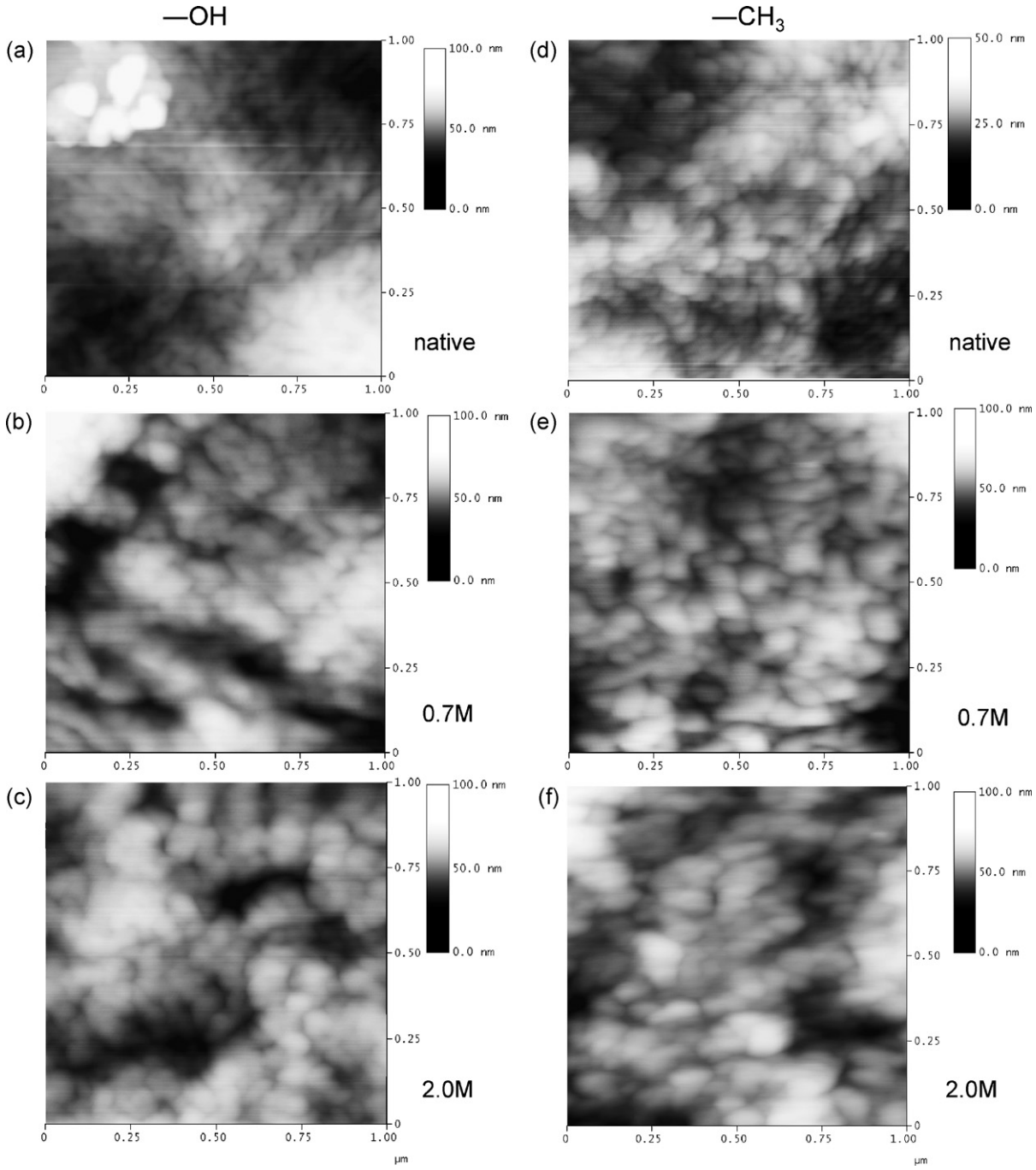

Fig. 4. Chemical force microscopy topography image of tapioca starch. Samples were prepared for imaging as described in Section 2. (a) Native, (b) 0.7 M HCl hydrolyzed, and (c) 2.0 M HCl hydrolyzed starch interaction with –OH probe; (d) native, (e) 0.7 M HCl hydrolyzed, and (f) 2.0 M HCl hydrolyzed starch interaction with $–CH_3$ probe.

of each sample were taken to verify the characteristic of the sample.

2.4. Preparation of CFM probe

Silicon nitride CFM probe was cleaned with H_2SO_4:H_2O_2 mixture (7:3, v/v) for 30 min at 50 °C, rinsed with deionized water, and stored in deionized water until silane attachment. –OH functional group was used after this cleaning process without further silane attachment because the cleaning process with H_2SO_4:H_2O_2 mixture had exposed the silanol group (–Si–OH).

For silane attachment, $–CH_3$ probe modification was conducted in a two-liter vacuum chamber equipped with a rotary vacuum pump. Petri dish filled with paraffin wax support was placed in the vacuum chamber and kept under vacuum for 2 h to degas the paraffin support. A 200 μl aliquot of silane was placed on the paraffin support and cleaned CFM probe attached to a glass slide was placed over the Petri dish. The chamber was pumped for another 2 h and sealed. The probe was kept under the silane vapor for 1 week, then washed with toluene, ethanol, and deionized water, and dried with nitrogen gas [28,29].

2.5. CFM sample preparation

CFM sample preparation was done by placing 0.01 g of the prepared starch granules onto a pre-wetted mica sheet attached on the sample stub. The excess starch granules were then blown-off with nitrogen gas at 200 psi leaving only granules that are bounded to the mica sheet.

2.6. Chemical force imaging

All images and chemical mapping data collection were performed using a scanning force microscope (Nanoscope IIIa Multimode, Veeco Digital Instrument). The cantilever has a nominal spring constant of 0.58 N m^{-1}. The mode of operation for all experiments was conducted using the contact mode, but with scanning at 90° to the orientation of the cantilever (Fig. 1). Scan size was 1 μm and scan rate was at 1 Hz.

3. Results and discussion

3.1. Amylopectin ratio increased from acid hydrolysis and surface disruption analysis with SEM

Fig. 2 shows a plot of the Am:Ap ratio of tapioca starch versus time following HCl hydrolysis. Amylopectin ratio increased with higher concentration of acid hydrolysis. Several previous work have investigated the Am:Ap ratio in relation to molecular weight [6,36–39]. Hydrolysis time of 3.5 h was chosen for further study because there was a significant difference in the Am:Ap ratio for both 0.7 M and 2.0 M of HCl hydrolysis. The two acid concentrations were widely used in modifying starch for various applications [1–6]. The effects of acid hydrolysis on starch surface could be studied from representative SEM micrographs as shown in Fig. 3. Micrograph of native starch showed the pristine surface of the granule itself. And between 30 min hydrolysis with 0.7 M and 2.0 M of HCl, it could be seen that 2.0 M hydrolysis had notable surface disruption compared to 0.7 M, as would be expected as the acid hydrolyzed away the amylose part.

3.2. Topography scanning force imaging

Fig. 4a–c shows topography images of –OH probe interaction with native, 0.7 M, and 2.0 M HCl hydrolyzed starch, respectively. Fig. 4d–f shows topography images of $–CH_3$ probe interactions with the three types of starch samples. Although, it was difficult to probe the exact same area while changing the –OH probe to $–CH_3$ probe, the experiment was performed with most care in order to probe the same position as possible. As seen in Fig. 4, all images showed very similar nodule-like structures that are blocklets of amylopectin. The topography and size of the blocklets were similar using either the –OH or the $–CH_3$ probes, this indicates similar scanning area and that the chemically modified SFM probes with organosilane did not reduce the *xy*-resolution of the probe or at least not detectable for the particular scan size. The $–CH_3$ probe should, however, show higher interaction to nonpolar domains of the blocklet compared with –OH probe [25–27]. But, the differences in the chemical domain could not be determined with the topography images.

3.3. Chemical force imaging of phosphate and carbon backbone

To detect probe–specimen chemical interaction, three images were collected simultaneously, namely, the topography image, the lateral force (LF)-trace image, and the LF-retrace image. LF-trace and LF-retrace images were collected in opposite scanning directions. Topography image was collected as comparison, giving information regarding the *z*-axis and also in determining the similarity of the scanned area and quality (shown in Fig. 4a–f). A post-image processing, trace-minus-retrace (TMR), was performed on LF-trace and LF-retrace images to correct for imaging that may have resulted from height differences. Fig. 5 shows a simulation demonstrating the concept of TMR in canceling out topography information and put forward only chemical interaction information. However, for large height variations, TMR was not applicable, as the appearance of the large objects in the top left hand images in Figs. 4a and 6a suggested that not all the topography effects had been removed.

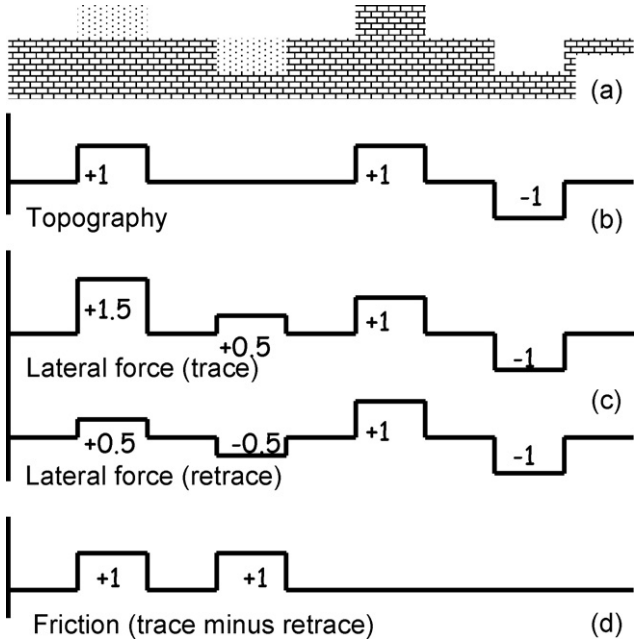

Fig. 5. Simulation of lateral force microscopy trace-minus-retrace (TMR) data processing. (a) Simulated surface with two types of materials having different chemical domains and areas with only height differences. (b) Topography profile of the simulated surface. (c) Lateral force (trace) and (retrace) profile where both chemical domains and height information are coupled together, and lateral force (trace) and (retrace) information have opposite signs. (d) Result of trace-minus-retrace profile, leaving only the chemical domain information.

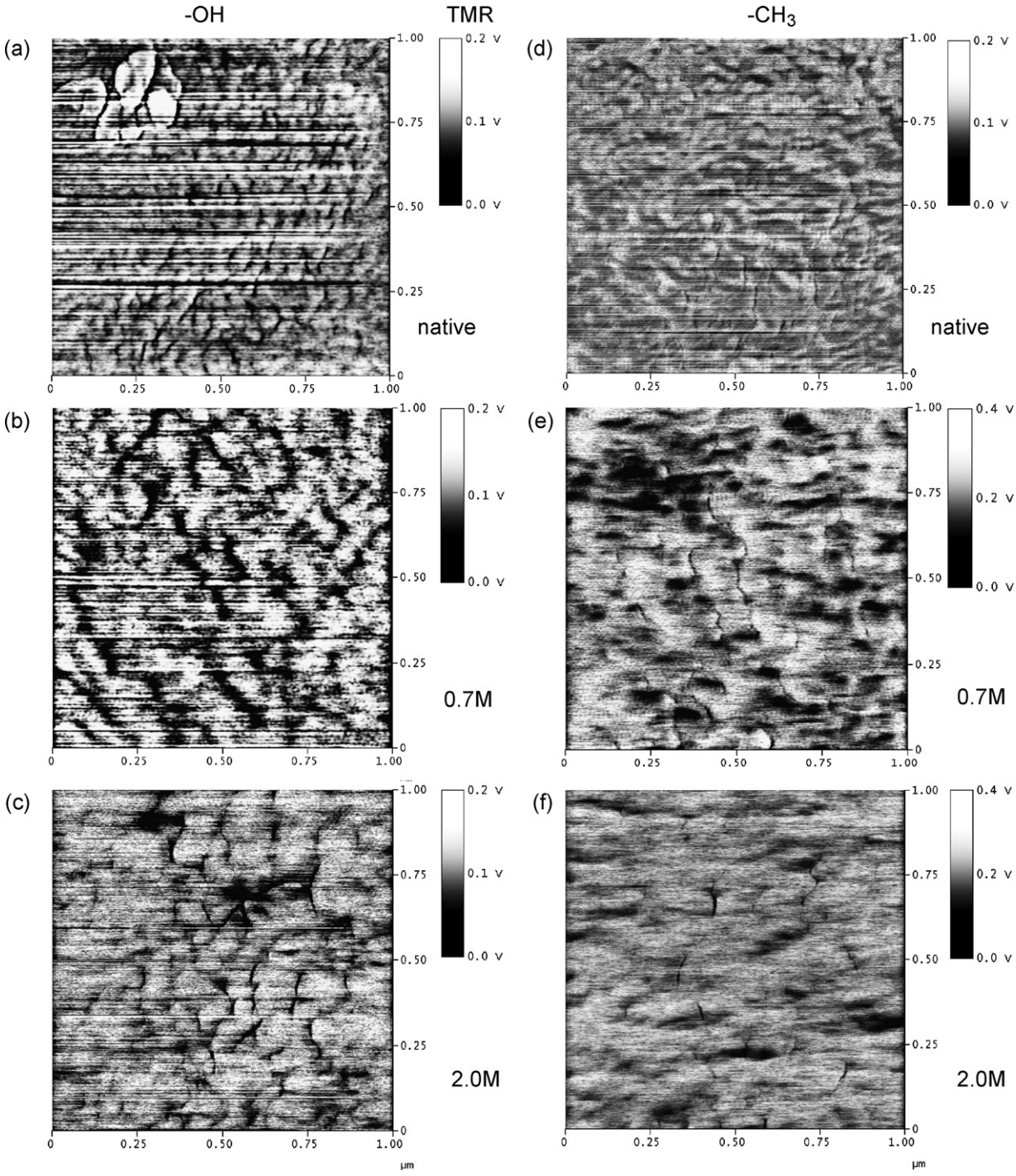

Fig. 6. Trace-minus-retrace (TMR) image. Samples were prepared for imaging as described in Section 2. (a) Native, (b) 0.7 M HCl hydrolyzed, and (c) 2.0 M HCl hydrolyzed starch interaction with –OH probe; (d) native, (e) 0.7 M HCl hydrolyzed, and (f) 2.0 M HCl hydrolyzed starch interaction with $–CH_3$ probe.

Fig. 6a–c shows TMR images of –OH probe interaction to native, 0.7 M, and 2.0 M HCl hydrolyzed starch, respectively. The size of the blocklet structure increased with higher acid concentration resulting from the exposure of the higher amylopectin ratio on the surface. Higher amylopectin ratio corresponded to higher phosphorus content [5,30–34]. *Dark areas* in TMR images were *not physical topography* grooves, but corresponded to regions of *reduced chemical interaction*. *Light areas* in the TMR images resulted from *strong chemical interaction* between –OH probes with the phosphate domains on the starch surface. Molecular friction between –OH probes and phosphate substrates had been shown to be higher than with carbon substrates [26]. This was because nonpolar–polar (–CH– ↔ –OH) van der Waal's interaction was found to be smaller than van der Waal's forces to similar pairs polar–polar interactions (–OH ↔ $–PO_{4–}^{+}$) [25]. Vegte and Hadziioannou [26] had given detailed study of various functionalized probe interactions including, $–CH_3$ and –OH probes to various substrates. The horizontal streak lines were artifacts inherent to the nature of the CFM technique.

Fig. 6d–f shows TMR image of $-CH_3$ probe interaction to native, 0.7 M HCl hydrolyzed, and 2.0 M HCl hydrolyzed starch, respectively. The blocklet structures were no longer observed, but instead the structures had plate-like sheet features. The $-CH_3$ probe mapped the interaction of the nonpolar carbon backbones of the glucose unit of the starch surface structure. The blocklet structures disappeared because the blocklet structures were predominantly phosphate domains in the amylopectin cluster that were not detected by the $-CH_3$ probe. These results indicated that the carbon backbone had plate-like structures while the phosphate domains were packed in blocklets of the amylopectin clusters on the starch surface.

4. Conclusions

The exterior structures of the acid hydrolyzed starch granules were chemically investigated with CFM to study the relationships of the surface molecular structures and the Am:Ap ratios. Of the increasing acid concentration for hydrolysis, the amylopectin ratio increased and exposed more of the phosphate blocklets. The phosphate domains were mapped as blocklets in the amylopectin clusters with the –OH probe. While the –CH probe revealed images of the carbon backbone of the glucose unit. The carbon backbone had a plate-like structure. The technique offered a potential route to mapping molecular or chemical entities on the surface of starch granules and, in the future, on the interior of sectioned starch granules.

Acknowledgements

This work was supported by The National Center for Genetic Engineering and Biotechnology (BIOTEC), The Thailand Research Fund (TRF), The Commission on Higher Education, Mahidol Research Grant, Postgraduate Education and Research Program in Chemistry (PERCH-CIC), and The Thai Center of Excellence for Physics (Integrated Physics Cluster). The facilities provided by the Nano-Imaging Unit, Faculty of Science, Mahidol University are also acknowledged.

References

[1] F. Brouillet, B. Bataille, L. Cartilier, Int. J. Pharm. 356 (2008) 52–60.
[2] H.J. Bae, D.S. Cha, W.S. Whiteside, H.J. Park, Food Chem. 106 (2008) 96–105.
[3] H. Wu, E.J. Heilweil, A.S. Hussain, M.A. Khan, Int. J. Pharm. 343 (2007) 148–158.
[4] H. Puchongkavarin, W. Bergthaller, S. Shobsngob, S. Varavinit, Starch/Stärke 55 (2003) 464–475.
[5] N. Atichokudomchai, S. Varavinit, Carbohydr. Polym. 53 (2003) 263–270.
[6] R. Hoover, Food Rev. Int. 16 (2000) 369–392.
[7] J. Chun, S. Lim, Y. Takeda, M. Shoki, Cereal Food. World 42 (1997) 813–819.
[8] D. French, in: R.L. Whistler, J.N. BeMiller, E.F. Paschal (Eds.), Starch Chemistry and Technology, 2nd ed., Academic Press, New York, 1984, pp. 183–247.
[9] T. Komiya, S. Nara, Starch/Stärke 38 (1986) 9–13.
[10] S. Vasudeva, S. Zakiuddin Ali, S. Divakar, Starch/Stärke 45 (1993) 59–62.
[11] N. Atichokudomchai, S. Shobsngob, P. Chinachoti, S. Varavinit, Starch/Stärke 53 (2001) 577–581.
[12] N.I. Abu-lail, T.A. Camesano, J. Microsc. 212 (2003) 217–238.
[13] A.A. Baker, M.J. Miles, W. Helbert, Carbohydr. Res. 330 (2001) 249–256.
[14] M.J. Ridout, A.P. Gunning, M.L. Parker, R.H. Wilson, V.J. Morris, Carbohydr. Polym. 50 (2002) 123–132.
[15] D.J. Gallant, B. Bouchet, P.M. Baldwin, Carbohydr. Polym 32 (1997) 177–191.
[16] P.M. Baldwin, M.C. Davies, C.D. Melia, Int. J. Biol. Macromol. 21 (1997) 103–107.
[17] N.H. Thomson, M.J. Miles, S.G. Ring, P.R. Shewry, A.S. Tatham, J. Vac. Sci. Technol. B 12 (1994) 1565–1568.
[18] P.M. Baldwin, R.A. Frazier, J. Adler, T.O. Glasbey, M.P. Keane, C.J. Roberts, S.J.B. Tendler, M.C. Davies, C.D. Melia, J. Microsc. 184 (1996) 75–80.
[19] A. Buleon, P. Colonna, V. Planchot, S. Ball, Int. J. Biol. Macromol. 23 (1998) 85–112.
[20] D. Saibene, K. Seetharaman, Starch/Stärke 60 (2008) 1–7.
[21] Z. Tüske, K. László, K. Pintye-Hódi, Starch/Stärke 59 (2007) 510–512.
[22] S.P. Cauvain, B.M. Gough, M.E. Whitehouse, Starch/Stärke 29 (1977) 91–95.
[23] A.C. Eliasson, K. Larsson, Y. Miezis, Starch/Stärke 33 (1981) 231–235.
[24] W. Nierle, A.W. El Bayâ, H.J. Kersting, D. Meyer, Starch/Stärke 42 (1990) 471–475.
[25] J.N. Israelachvili, Intermolecular and Surface Forces, 2nd ed., Academic Press, New York, 1992, p. 50.
[26] E.W. van der Vegte, G. Hadziioannou, Langmuir 13 (1997) 4357–4368.
[27] S. Termnak, K. Sintasanai, T. Nipithakul, T. Amornsakchai, D. Triampo, Chin. J. Polym. Sci. 26 (2008) 275–283.
[28] T. Nakagawa, K. Ogawa, T. Kurumizawa, S. Ozaki, Jpn. J. Appl. Phys. 32 (1993) L249.
[29] T. Nakagawa, K. Ogawa, T. Kurumizawa, J. Vac. Sci. Technol. B 12 (1994) 2215.
[30] M.Z. Sitohy, M.F. Ramadan, Starch/Stärke 53 (2001) 27–34.
[31] J. Jane, T. Kasemsuwan, J.F. Chen, Cereal Food. World 41 (1996) 827–832.
[32] T.J. Schoch, J. Am. Chem. Soc. 64 (1942) 2957–2961.
[33] S. Tabata, K. Nagata, S. Hizukuri, Starch/Stärke 27 (1975) 333–335.
[34] J. Jane, A. Xu, M. Radosavljevic, P.A. Seib, Cereal Chem. 69 (1992) 405–409.
[35] B.O. Juliano, Cereal Sci. Today 16 (1971) 334–339.
[36] Y. Song, J. Jane, Carbohydr. Polym. 41 (2000) 365–377.
[37] L.M.K. Ferrini, T.S. Rocha, I.M. Deminate, C.M.L. Franco, Starch/Starke 60 (2008) 417–425.
[38] D. Kuakpetoon, Y.J. Wang, Carbohydr. Res. 342 (2007) 2253–2263.
[39] D. Kuakpetoon, Y.J. Wang, Carbohydr. Res. 343 (2008) 90–100.